

Learning Dynamic Graph Representations through Timespan View Contrasts

Yiming Xu^a, Zhen Peng^{a,*}, Bin Shi^a, Xu Hua^a, Bo Dong^b

^a*School of Computer Science and Technology, Xi'an Jiaotong University, P.R. China*

^b*School of Distance Education, Xi'an Jiaotong University, P.R. China*

Abstract

The rich information underlying graphs has inspired further investigation of unsupervised graph representation. Existing studies mainly depend on node features and topological properties within static graphs to create self-supervised signals, neglecting the temporal components carried by real-world graph data, such as timestamps of edges. To overcome this limitation, this paper explores how to model temporal evolution on dynamic graphs elegantly. Specifically, we introduce a new inductive bias, namely temporal translation invariance, which illustrates the tendency of the identical node to keep similar labels across different timespans. Based on this assumption, we develop a dynamic graph representation framework CLDG that encourages the node to maintain locally consistent temporal translation invariance through contrastive learning on different timespans. Except for standard CLDG which only considers explicit topological links, our further proposed CLDG++ additionally employs graph diffusion to uncover global contextual correlations between nodes, and designs a multi-scale contrastive learning objective composed of local-local, local-global, and global-global contrasts to enhance representation capabilities. Interestingly, by measuring the consistency between different timespans to shape anomaly indicators, CLDG and CLDG++ are seamlessly integrated with the task of spotting anomalies on dynamic graphs, which has broad applications in many high-impact domains, such as finance, cybersecurity, and healthcare. Experiments demonstrate that CLDG and

*Corresponding author.

Email addresses: xym0924@stu.xjtu.edu.cn (Yiming Xu), zhenpeng27@outlook.com (Zhen Peng), shibin@xjtu.edu.cn (Bin Shi), huaxu@stu.xjtu.edu.cn (Xu Hua), dong.bo@xjtu.edu.cn (Bo Dong)

CLDG++ both exhibit desirable performance in downstream tasks including node classification and dynamic graph anomaly detection. Moreover, CLDG significantly reduces time and space complexity by implicitly exploiting temporal cues instead of complicated sequence models. The code and data are available at <https://github.com/yimingxu24/CLDG>.

Keywords:

Dynamic Graph, Graph Representation Learning, Contrastive Learning, Graph Anomaly Detection

1. Introduction

Graph data is prevalent in various real-world domains. In recent years, research on high-quality representation learning for graph-structured data has attracted much attention (Xu et al., 2025e,a). Traditional representation learning methods often struggle to handle the complexity of graph-structured data effectively. In contrast, graph neural networks (GNNs) provide a novel perspective for modeling and analyzing graph data. GNNs have demonstrated remarkable performance in a wide range of applications, including recommender systems (Wu et al., 2020; Zhou et al., 2024), combinatorial optimization (Li et al., 2018; Cappart et al., 2021), traffic prediction (Derrow-Pinion et al., 2021; Fan et al., 2024), and risk management (Zheng et al., 2023; Song et al., 2024; Xu et al., 2025d).

Despite the empirical success, most existing GNN methods typically focus on static graphs and heavily rely on supervised learning paradigms. It is undeniable that real-world graph data inherently carries temporal information, such as timestamps of edges. The loss of information caused by ignoring these temporal components would lead to performance corruption. In addition, acquiring sufficient and high-quality labels in graph data necessitates rich domain knowledge and experience, which leads to expensive labor and time costs. Even sometimes we cannot access label signals due to data privacy and security issues. Thus, exploring high-quality dynamic graph representation learning techniques in an unsupervised manner becomes an important and challenging task.

By conducting empirical analysis on many collected dynamic graphs, as shown in Figure 1, we find an interesting observation that the prediction labels of the same node tend to keep similarity in different timespans regardless of the encoder employed like GCN (Kipf and Welling, 2016), GAT (Veličković

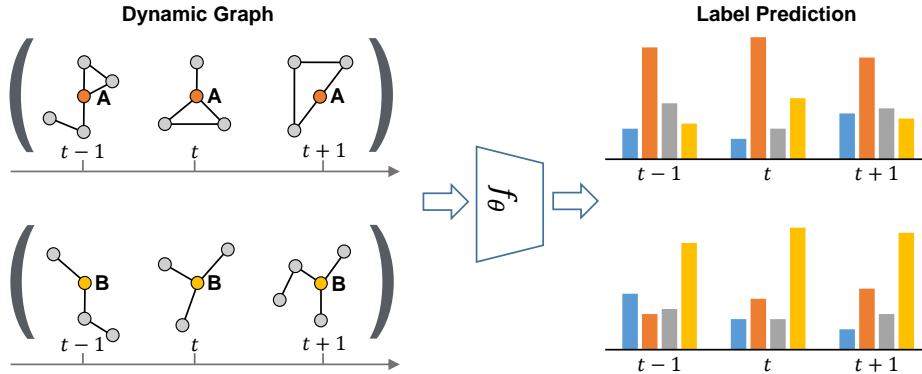


Figure 1: Illustration of our basic idea. In the collected datasets (details are demonstrated in Section 5.1.1), an interesting observation is that the semantics and labels learned by the same node tend to be similar no matter what encoder is used at different timespans of the dynamic graph. We refer to this observation as temporal translation invariance. Based on temporal translation invariance, we claim that the features of node A, on different timespan should be similar and pull apart the features of other nodes, such as B.

et al., 2017) or MLP (McCulloch and Pitts, 1943). We refer to this phenomenon on dynamic graphs as temporal translation invariance, which is supported by a wealth of intuitions. For instance, most researchers are deeply immersed and dedicated to specific fields throughout their careers. Similarly, the business scope of a company remains almost unchanged in tax transaction networks. The assumption of temporal translation invariance opens the door for us to explore semantic temporal cues through contrastive learning for dynamic graph representation. Specifically, we employ diverse timespan views to create contrastive pairs. By maximizing the semantic mutual information (MI) between identical nodes in contrast views, we can derive informative node representations without the dependence on labeled data. Treating views of different timespans as contrastive pairs is a more graceful way that does not require manual trial-and-error, cumbersome searches, or expensive domain knowledge for augmentation selection (Xia et al., 2022).

To take advantage of the temporal translation invariance assumption, in this paper, we introduce a Contrastive Learning framework on Dynamic Graphs (CLDG) that is conceptually straightforward and highly effective. To begin with, we employ a timespan view sampling strategy to generate multiple views from continuous dynamic graphs. Then the encoder and projection head are utilized to learn node representations, which is accomplished by effectively aggregating neighborhood information from the adjacency ma-

trix in the timespan view. CLDG treats the semantics of the same node in different timespan views as positive pairs to encourage the representation of the same node in each timespan view to be similar. Note that the adjacency matrix only captures local information from direct neighborhoods and lacks the exploration of implicit topological correlations, which would limit the performance of downstream tasks (Gasteiger et al., 2019; Hassani and Khasahmadi, 2020). For example, in anomaly detection scenarios, fraudsters often deliberately conceal their social relationships through camouflage to reduce their suspicion and evade detection (Dou et al., 2020; Ma et al., 2021). Therefore, to maximize the preservation and extraction of global information in graphs to promote high performance in downstream tasks, we introduce the extended CLDG++ in this work. By incorporating graph diffusion (Page et al., 1999; Kondor and Lafferty, 2002) to simulate the propagation process of information on the graph, CLDG++ enlarges the receptive field and effectively models the implicit and global topology of each sampled timespan view. Moreover, we specifically designed a multi-scale contrastive learning objective composed of local-local, local-global, and global-global contrasts for CLDG++ to enhance its simultaneous capture of local and global information. Note that rapid or sudden changes in node features or structures on dynamic graphs mostly imply deviations in data patterns and are closely related to anomalies. For example, abnormal companies may suddenly trade in commodities that deviate significantly from their established lines of business or experience a sudden surge in trading activity over a short period. Based on the intuition that anomalies usually violate the assumption of temporal translation invariance, we create an anomaly indicator by capturing contextual consistency and stability in temporal components, which empowers CLDG and its extension to efficiently spot anomalies on dynamic graphs. The main contributions are summarized as follows:

- **Assumption:** We propose a novel inductive bias named temporal translation invariance on dynamic graphs. Based on this assumption, we generalize the idea of contrastive learning to dynamic graph representation learning by treating nodes in different timespans as contrastive pairs.

- **Algorithms:** We propose an efficient contrastive learning method on dynamic graphs to perform representation learning in unsupervised scenarios. In addition to CLDG based on local topological views, we also present its extended version CLDG++ which combines local and global views to derive more comprehensive representations. More interestingly, we seamlessly integrate CLDG/CLDG++ with the anomaly detection task by shaping an

anomaly indicator to catch violations of temporal translation invariance.

• **Downstream Applications:** We corroborate the effectiveness of CLDG and CLDG++ on node classification and dynamic graph anomaly detection tasks. The experiments showcase the remarkable potential of our methods in leveraging large-scale unlabeled dynamic graph data.

Our preliminary work is published in (Xu et al., 2023). Compared to the previous version, we first introduce a novel variant called CLDG++, which leverages Personalized PageRank (PPR) (Page et al., 1999) and heat kernel (Kondor and Lafferty, 2002) to uncover the global contextual relationships and the degree of interaction between nodes in the graph. This approach goes beyond the limited local receptive field characterized by simple binary connections in the adjacency matrix, allowing us to capture more comprehensive insights into implicit links and global topological properties. For example, recovering social relations maliciously concealed by fraudsters facilitates exposing underlying anomalous behaviors in anomaly detection scenarios. To effectively capture local and global information in large-scale unlabeled data, we design a multi-scale contrastive learning objective composed of local-local, local-global, and global-global contrasts accordingly. To promote the application research of the proposed representation model, we create an anomaly indicator to catch violations of temporal translation invariance based on the intuition that rapid or sudden changes in node features or structures on dynamic graphs are closely related to anomalies. Then, CLDG and CLDG++ are successfully applied to unsupervised dynamic graph anomaly detection, which has broad applications in many high-impact domains but has received relatively little scrutiny.

2. Related Work

2.1. Contrastive Learning on Graphs

Supervised and semi-supervised learning still dominate in graph neural networks (Feng et al., 2020; Wang et al., 2020; Dornaika et al., 2023; Han et al., 2023). However, the graph itself is an abstraction of the real world, and graph data suffers from the problems of lack of labels and difficulty in labeling. Recently, contrastive learning is highly successful in computer vision (CV) and natural language processing (NLP) (Wu et al., 2018; Van den Oord et al., 2018; He et al., 2020; Chen et al., 2020; Grill et al., 2020; Gao et al., 2021). Inspired by the above methods, there are some works that extend contrastive learning to graphs. DGI (Velickovic et al., 2019) extends deep

InfoMax (Hjelm et al., 2018) to graphs and maximizes MI between global graph embeddings and local node embeddings. GraphCL (You et al., 2020) proposes a novel graph contrastive learning framework that systematically explores the performance impact of various combinations of four different data augmentations. GCA (Zhu et al., 2021) and GRACE (Zhu et al., 2020) pay more attention to the graph data augmentation and propose adaptive data augmentation schemes on topology and node attributes. MVGRL (Hassani and Khasahmadi, 2020) creates another view for the graph by introducing graph diffusion (Gasteiger et al., 2019). A discriminator contrasts node representations from one view with graph representation of another view and vice versa, and scores the agreement between representations, which is used as the training signal. CCA-SSG (Zhang et al., 2021) first generates two views of the input graph through data augmentation, and then uses the idea based on Canonical Correlation Analysis (CCA) to maximize the correlation between the two views and encourages different feature dimensions to capture distinct semantics. However, the above methods have two problems: (1) They require two views generated by corrupting the original graph, such as node dropping, edge perturbation, and attribute masking, etc. Inappropriate data augmentation may introduce noisy information resulting in semantic and label changes. (2) They are designed for static graphs. Applying contrastive learning directly to dynamic graphs is not straightforward.

2.2. Representation Learning on Dynamic Graphs

Traditionally, the static graph representation problem is intensively studied by researchers and a variety of effective works are proposed (Kipf and Welling, 2016; Veličković et al., 2017; Chien et al., 2021; Zhao et al., 2023; Jiang et al., 2023; Xu et al., 2025b). However, real-world networks all evolve over time, which poses important challenges for learning and inference. Therefore, there has been an increasing amount of research on dynamic graph representations recently (Ma et al., 2023). According to the modeling method of the dynamic graph, these works can be roughly divided into discrete-time methods (Goyal et al., 2018; Sankar et al., 2020; Xu et al., 2020; Pareja et al., 2020; Xue et al., 2020; Wang et al., 2021) and continuous-time methods (Zuo et al., 2018; Kumar et al., 2019; Trivedi et al., 2019; Lu et al., 2019).

Discrete-time Methods DynGEM (Goyal et al., 2018) uses a deep autoencoder to capture the connectivity trends in a graph snapshot at any time step. DySAT (Sankar et al., 2020) generates dynamic node representations through

self-attention along both structural and temporal. TGAT (Xu et al., 2020) uses the self-attention mechanism and proposes a time encoding technique based on the theorem of Bochner. STAR (Xu et al., 2019), DyHATR (Xue et al., 2020), dyngraph2vec (Goyal et al., 2020) and TemGNN (Wang et al., 2021) use different encoders (such as GCN (Kipf and Welling, 2016), autoencoder (Baldi, 2012), hierarchical attention model, etc.) to extract the features of each time snapshot respectively, and then introduce sequence models such as LSTM (Hochreiter and Schmidhuber, 1997) and GRU (Cho et al., 2014) to capture timing information.

Continuous-time Methods HTNE (Zuo et al., 2018) proposes a Hawkes process based temporal network embedding method to capture the influence of historical neighbors on the current neighbors. JODIE (Kumar et al., 2019) uses a coupled RNN architecture to update the embedding of users and items at every interaction. DyRep (Trivedi et al., 2019) builds a two-time scale deep temporal point process approach to capture the continuous-time fine-grained temporal dynamics processes. M²DNE (Lu et al., 2019) designs a temporal attention point process to capture the fine-grained structural and temporal properties in micro-dynamics, and defines a dynamics equation to impose constraints on the network embedding in macro-dynamics.

However, existing dynamic graph work still suffers from at least one of the following limitations: (1) Most sequence models such as RNN-like methods have high time costs and space complexity, and are not easily parallelized. This hinders the scaling of existing dynamic graph models to large-scale graphs. (2) Most models by reconstructing future states or temporal point processes or sequences may learn noisy information as they try to fit each new interaction in turn. (3) The temporal regularizer is similar to contrastive learning without negative examples, which forces the node representation to smooth from adjacent snapshots. However, a potential problem of this approach is the existence of completely collapsed solutions.

2.3. Anomaly Detection on Graphs

In recent years, the widespread application of graphs in domains such as finance, social networks, security, and medicine has attracted considerable interest in research on graph anomaly detection (Zheng et al., 2023; Shi et al., 2023). Graph anomaly detection aims to identify abnormal objects (i.e., nodes, edges, and sub-graphs) that deviate from the majority in graph data, which plays a crucial role in several high-impact applications,

including financial fraud detection, fake account detection, and network intrusion detection (Ma et al., 2021; Zhang et al., 2024; Xu et al., 2025c). At present, most existing works focus on node-level detection. For instance, DOMINANT (Ding et al., 2019a) detects anomalies by measuring the reconstruction errors of nodes from both the structural and attribute perspectives after GCN. AEGIS (Ding et al., 2021) first learns anomaly-aware node representations through an autoencoder network, then employs generative adversarial learning to detect anomalies among data. CoLA (Liu et al., 2021a) first introduces contrastive learning to effectively detect node anomalies in the graph, by measuring whether the target node matches its positive and negative neighbor sample pairs. Based on CoLA, ANEMONE (Jin et al., 2021) adds patch-level (i.e., node versus node) consistency to further estimate the anomaly score of nodes. The subgraph-subgraph contrast first proposed by GRADATE (Duan et al., 2023) is combined with the widely used node-subgraph and node-node contrasts to capture anomaly information. However, the above methods all work under the settings of static graphs. In contrast, anomaly detection on dynamic graphs has received relatively little scrutiny. Only a few works have explored dynamic graph scenarios with temporal information. NetWalk (Yu et al., 2018) utilizes random walks to generate node embeddings and then flag anomalies based on a dynamic clustering model. TADDY (Liu et al., 2021b) detects edge anomalies through a dynamic graph transformer model. SAD (Tian et al., 2023) proposes a semi-supervised dynamic graph anomaly detection framework, which also uses a time-equipped memory bank and pseudo-label contrastive learning to exploit the potential of unlabeled samples.

In summary, the existing research on anomaly detection in dynamic graphs is limited. Our study is committed to combining unsupervised dynamic graph representation methods with graph anomaly detection tasks to provide new ideas for successfully identifying dynamic graph anomalies.

3. Preliminaries

This section presents the necessary notations, definitions, and studied problems in this paper. The main notations are summarized in Table 1.

3.1. Dynamic Graph Modeling

The existing dynamic graph modeling methods can be roughly divided into two categories (Xue et al., 2022; Kazemi et al., 2020): discrete-time

Table 1: Notations and Descriptions.

Notations	Descriptions
\mathcal{G}	A dynamic graph
\mathcal{V}	The set of nodes in \mathcal{G}
\mathcal{E}	The set of edges in \mathcal{G}
τ	The temperature parameter
s	The view timespan factor
v	The number of views sampled
$a, \mathbf{a}, \mathbf{A}$	Scalar, vector, matrix
$\mathbb{R}_{\text{sample}}(\cdot, \cdot, \cdot)$	Timespan view sampling function

dynamic graph and continuous-time dynamic graph. We formally define two modeling methods as follows:

Definition 1 (Discrete-time Dynamic Graph). *A discrete-time dynamic graph (DTDG) is a sequence of network snapshots within a given time interval. Formally, we define a DTDG as a set $\{\mathcal{G}^1, \mathcal{G}^2, \dots, \mathcal{G}^T\}$ where $\mathcal{G}^t = \{\mathcal{V}^t, \mathcal{E}^t\}$ is the graph at snapshot t , \mathcal{V}^t is the set of nodes in \mathcal{G}^t , and $\mathcal{E}^t \subseteq \mathcal{V}^t \times \mathcal{V}^t$ is the set of edges in \mathcal{G}^t .*

Definition 2 (Continuous-time Dynamic Graph). *A continuous-time dynamic graph (CTDG) is a network with edges and nodes annotated with timestamps. Formally, we define a CTDG as $\mathcal{G} = \{\mathcal{V}^T, \mathcal{E}^T, \mathcal{T}\}$ where $\mathcal{T} : \mathcal{V}, \mathcal{E} \rightarrow \mathbb{R}^+$ is a function that maps each node and edge to a corresponding timestamp.*

3.2. Problem Formulation

The objective of this paper is to design a dynamic graph representation method. The mathematical formulation of this problem could be defined as:

Problem 1 (Representation Learning on Dynamic Graph). *Given a dynamic graph $\mathcal{G} = \{\mathcal{V}, \mathcal{E}, \mathcal{T}\}$, our goal is to learn a mapping function $f : v_i \rightarrow \mathbf{z}_i \in \mathbb{R}^d$, where $d \ll |\mathcal{V}|$, and \mathbf{z}_i is the embedded vector that preserves both temporal and structural information of vertex v_i .*

With the aforementioned notations, we formalize the problem of dynamic graph anomaly detection as follows:

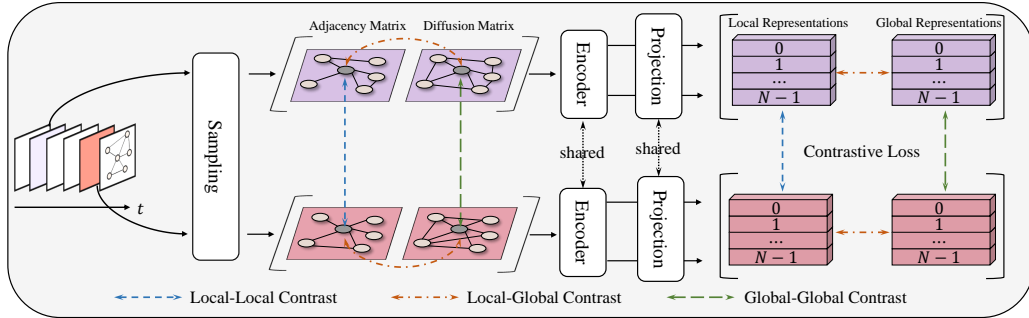


Figure 2: The architecture of the CLDG++. Given an input graph, we first sample multiple views through a timespan view sampling layer. Subsequently, each view generates a diffusion matrix through graph diffusion, where the adjacency matrix and diffusion matrix offer local and global perspectives of the graph structure, respectively. Then, the adjacency and diffusion matrices of the views are fed into the encoder to generate node embeddings, and a projection head is utilized to map the embeddings into the space of the contrastive loss. Finally, CLDG trains the model by maintaining the temporal translation invariance between local-local contrast, while CLDG++ adds both local-global contrast and global-global contrast to capture both local and global topological properties.

Problem 2 (Anomaly Detection on Dynamic Graph). *Given a dynamic graph \mathcal{G} , the goal of anomaly detection is to learn an anomaly score function f to calculate the anomaly score $s_i = f(v_i)$ of each node. The anomaly score s_i measures the degree of abnormality for node v_i . A larger anomaly score means that it is more likely to be anomalous.*

4. Proposed Method

In this section, we propose a new unsupervised dynamic graph representation learning method CLDG++, whose framework overview and workflow are shown in Figure 2. It consists of five major lightweight components: timespan view sampling layer, graph diffusion layer, base encoder, projection head and contrastive loss function. To begin with, the view sampling layer extracts the temporally-persistent signals. Then, the global view is captured through the graph diffusion layer. Furthermore, the base encoder learns the local and global representations, and the projection head maps the representations into the space of the contrastive loss. Finally, the contrastive loss function is used to maintain the temporal translation invariance of the local-local, local-global, and global-global.

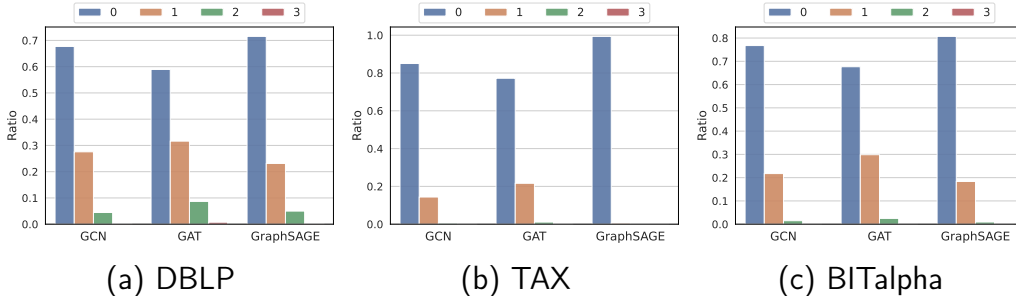


Figure 3: The ratio of the number of times the predicted node label has changed across timespans.

4.1. Temporal Translation Invariance

To explore the properties of dynamic graphs, we perform some empirical studies. Specifically, we first process dynamic graph datasets \mathcal{G} by splitting each of them into many timespans $\{\mathcal{G}^1, \mathcal{G}^2, \dots, \mathcal{G}^T\}$ (the specific datasets described in Section 5.1.1), where we set T to 4. For each timespans, we train common GNN encoders with the same architecture but without shared weights, where we choose three GNN encoders: GCN, GAT and GraphSAGE. The trained model is then used to predict the node labels. We calculate the ratio of the number of times the predicted node label changed over the timespan on three representative datasets (referred to as DBLP, TAX, and BITalpha), as illustrated in Figure 3. For example, a change count of 0 indicates consistent label predictions across all four timespans, and the Y-axis indicates the ratio of nodes demonstrating this behavior relative to the total number of nodes. An interesting observation is that regardless of the encoder used for training, the prediction labels of the same node tend to be similar in different timespans. We refer to this phenomenon as temporal translation invariance.

Under the assumption of temporal translation invariance, an unsupervised opportunity and pathway are provided to more elegantly exploit the supplementary temporal cues inherent in dynamic graphs. We utilize different timespan views to construct contrastive pairs. Specifically, we treat the semantics of the same node in different timespan views as positive pairs, pulling closer the representation of the same node in each timespan view, and pulling apart the representation of different nodes. This method effectively utilizes temporal information while avoiding noisy information caused

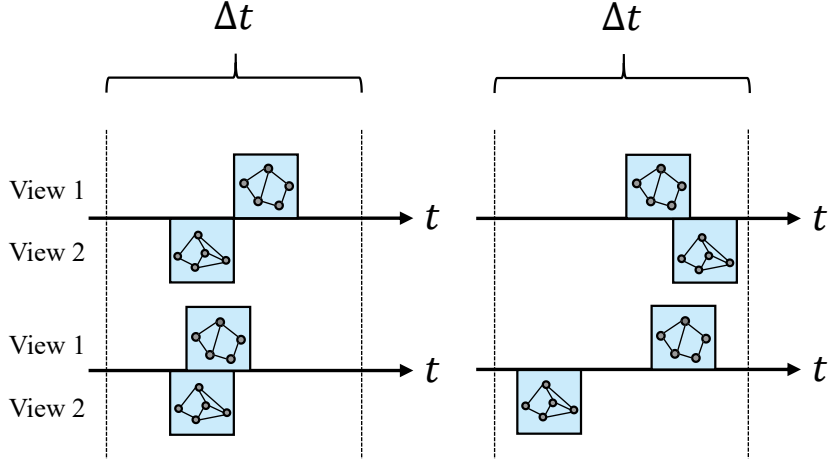


Figure 4: Four candidate timespan view sampling strategies.

by graph data augmentation techniques, such as node dropping, edge perturbation, and attribute masking commonly used in existing graph contrastive learning methods.

4.2. Timespan View Sampling Layer

Based on temporal translation invariance, we utilize different timespan views as contrastive pairs. However, how to specifically choose appropriate timespans is still an open question. First, it is intuitive that the interval distance between different timespan views may affect the contrastive learning results. In the case of two timespan views, if more temporal overlap exists between two views, they theoretically share more similar semantic contexts, but this may lead to over-simplified tasks. If two views are separated for a long time, they may have completely different neighbors and may no longer share the same semantic context. In addition, how to choose the appropriate number and size of timespan views is also to be studied. Therefore, we design four different timespan view sampling strategies to explore the optimal view interval distance selection, as shown in Figure 4. The main difference between each strategy is the rate of physical temporal overlap, thereby sharing different semantic contexts. Meanwhile, each sampling strategy considers both the number and size of views. Next, we formally define the timespan view sampling layer.

Specifically, given a continuous-time dynamic graph \mathcal{G} , we first define that the overall timespan of graph \mathcal{G} is $\Delta t = \max(\mathcal{T}) - \min(\mathcal{T})$. Then, we set two

factors v, s to control the number and size of the sampling timespan views respectively, i.e., v views are sampled for each strategy and the timespan of each view is $\Delta t/s$, and $v, s \in \mathbb{N}^*$ are hyperparameters that can be set according to the actual physical implication of the graph and the density of the graph. Finally, the timespan view sampling strategy can be formulated as:

$$(\mathcal{T}_1, \dots, \mathcal{T}_v) = \mathbb{R}_{\text{sample}}(s, v, \Delta t), \quad (1)$$

where $\mathcal{T}_i \in [\min(\mathcal{T}) + \frac{\Delta t}{2s}, \max(\mathcal{T}) - \frac{\Delta t}{2s}]$, $\forall i \in [1, v]$, and $\mathbb{R}_{\text{sample}}(\cdot, \cdot, \cdot)$ returns a sample time tuple.

We obtain v timespan views, i.e., $\tilde{\mathcal{G}}_1, \tilde{\mathcal{G}}_2, \dots, \tilde{\mathcal{G}}_v$, according to the sample time tuples $(\mathcal{T}_1, \dots, \mathcal{T}_v)$, where $\tilde{\mathcal{G}}_i$ retains all edges of \mathcal{G} in a specific timeframe $[\mathcal{T}_i - \frac{\Delta t}{2s}, \mathcal{T}_i + \frac{\Delta t}{2s}]$. Specifically, the sample time tuple can be generated by four different strategies. We formally define four sampling strategies by the time difference between \mathcal{T}_i in the sample time tuple and its predecessor \mathcal{T}_{i-1} and successor \mathcal{T}_{i+1} .

Sequential Sampling Strategy. This strategy first divides the dynamic graph into s timespan views, with no intersection between each view, and then randomly samples v unduplicated views, where $v \leq s$. This strategy is similar to the processing method of DTDG, which can be directly used in DTDG.

$$|\mathcal{T}_i - \mathcal{T}_{i\pm 1}| = \alpha \frac{\Delta t}{s}, \quad (2)$$

where $\alpha \in \mathbb{N}^*$, the time difference between any two views is an integer multiple of the timespan of the view.

High Overlap Rate Sampling Strategy. The v views sampled by this strategy are interdependent. We set an overlap rate of 75%, that is, the time between the sampled dynamic graphs $\tilde{\mathcal{G}}_i$ and $\tilde{\mathcal{G}}_{i\pm 1}$ corresponding to \mathcal{T}_i and $\mathcal{T}_{i\pm 1}$ has a 75% overlap.

$$|\mathcal{T}_i - \mathcal{T}_{i\pm 1}| = \frac{\Delta t}{4s}, \quad (3)$$

where \mathcal{T}_1 is limited by $[\min(\mathcal{T}) + \frac{\Delta t}{2s}, \max(\mathcal{T}) - \frac{(2+v)\cdot\Delta t}{4s}]$ and random sampling in each epoch, assuming that $\mathcal{T}_1 < \mathcal{T}_i < \mathcal{T}_v$ is satisfied in the sampled time tuple. Then \mathcal{T}_2 to \mathcal{T}_v are obtained according to Eq. 3.

Low Overlap Rate Sampling Strategy. The v views sampled by this strategy are interdependent. We set an overlap rate of 25%, which means that

the time between the sampled dynamic graphs $\tilde{\mathcal{G}}_i$ and $\tilde{\mathcal{G}}_{i\pm 1}$ corresponding to \mathcal{T}_i and $\mathcal{T}_{i\pm 1}$ has a 25% overlap.

$$|\mathcal{T}_i - \mathcal{T}_{i\pm 1}| = \frac{3\Delta t}{4s}, \quad (4)$$

where $\mathcal{T}_1 \in \left[\min(\mathcal{T}) + \frac{\Delta t}{2s}, \max(\mathcal{T}) - \frac{(2+3v)\cdot\Delta t}{4s} \right]$ and random sampling in each epoch, assuming that $\mathcal{T}_1 < \mathcal{T}_i < \mathcal{T}_v$ is satisfied in the sampled time tuple. Then \mathcal{T}_2 to \mathcal{T}_v are obtained according to Eq. 4.

Random Sampling Strategy. $\mathbb{R}_{\text{sample}}(\cdot, \cdot, \cdot)$ randomly returns a set of sample time tuples, where $\forall i$ satisfies $\mathcal{T}_i \in \left[\min(\mathcal{T}) + \frac{\Delta t}{2s}, \max(\mathcal{T}) - \frac{\Delta t}{2s} \right]$. The dynamic graphs $\tilde{\mathcal{G}}_i$ and $\tilde{\mathcal{G}}_j$ sampled corresponding to \mathcal{T}_i and \mathcal{T}_j may not overlap or partially overlap in time.

$$|\mathcal{T}_i - \mathcal{T}_{i\pm 1}| \in \left[0, \Delta t - \frac{\Delta t}{s} \right]. \quad (5)$$

Finally, the timespan view sampling layer samples V graph views in each training epoch, defined as $\{\tilde{\mathcal{G}}_1, \tilde{\mathcal{G}}_2, \dots, \tilde{\mathcal{G}}_V\}$ and $\tilde{\mathcal{G}}_i = \{\mathbf{X}_i, \mathbf{A}_i\}$, where \mathbf{X}_i and \mathbf{A}_i are the feature matrix and adjacency matrix of the i -th view.

4.3. Graph Diffusion Layer

Based on the above sampling strategy, we transform the original dynamic graph into timespan views, which define the topology of each view by the adjacency matrix. However, adjacency matrices only describe local information about simple binary connectivity from direct neighborhoods (Gasteiger et al., 2019; Hassani and Khasahmadi, 2020), and lack the consideration of implicit topological correlations, which would limit the performance of downstream tasks. In contrast, preserving and extracting as much global information as possible from graphs facilitates high-quality representation learning. We introduce two popular instantiations of generalized graph diffusion, PPR (Page et al., 1999) and heat kernel (Kondor and Lafferty, 2002) to uncover the global contextual relationships and the degree of interaction between nodes in the graph by simulating the propagation process of information on the graph. As shown in Figure 5, we visualize the adjacency matrices of the Florentine families graph (Breiger and Pattison, 1986) and the Davis Southern women social network (Davis et al., 1941), and the diffusion matrix generated by PPR, respectively. It is obvious from Figure 5b and Figure 5d that the diffusion matrix depicts more potential relationships between nodes, eliminating

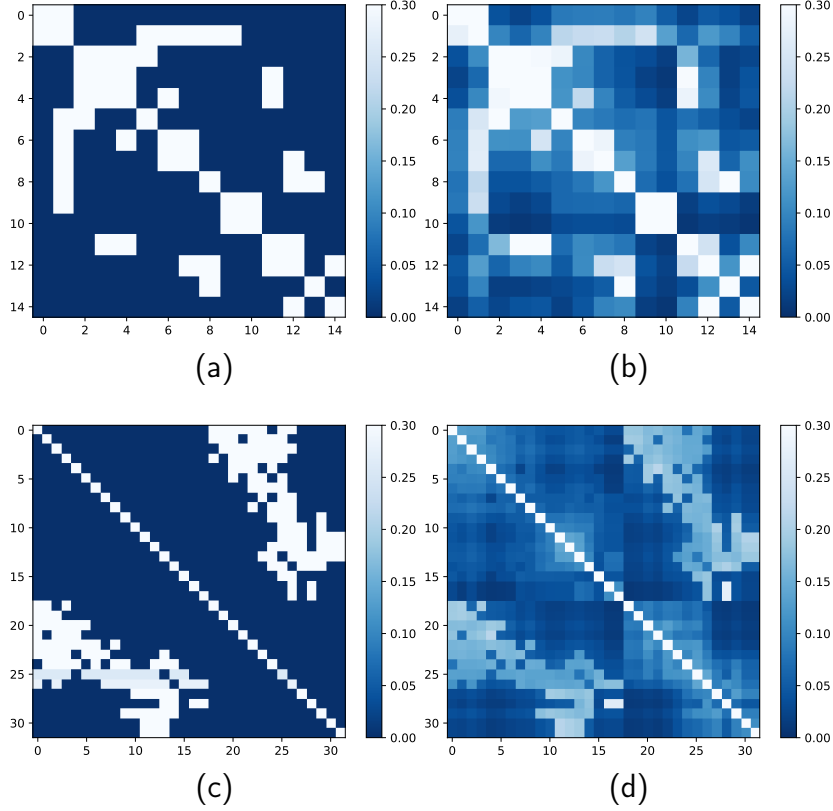


Figure 5: The heatmaps (a) and (c) of the normalized adjacency matrix, and the heatmaps (b) and (d) of the normalized diffusion matrix are visualized for the Florentine families graph (Breiger and Pattison, 1986) and the Davis Southern women social network (Davis et al., 1941), respectively.

the restriction of using only direct neighbors. By aggregating information from larger neighbors within the diffusion matrix, the model is enabled to learn global semantic information. Mathematically, the closed-form solution of the PPR and heat kernel is defined as:

$$\mathbf{S}^{\text{PPR}} = \alpha (\mathbf{I}_n - (1 - \alpha)\mathbf{D}^{-1/2}\mathbf{A}\mathbf{D}^{-1/2})^{-1}, \quad (6)$$

$$\mathbf{S}^{\text{heat}} = \exp(t\mathbf{A}\mathbf{D}^{-1} - t), \quad (7)$$

where \mathbf{D} is the degree matrix of \mathbf{A} . α denotes teleport probability in a random walk and t is diffusion time. For the V local timespan views sampled,

we generate corresponding global diffusion views $\{\mathbf{S}_1, \mathbf{S}_2, \dots, \mathbf{S}_V\}$.

4.4. Base Encoder Layer

For local and global timespan views, to ensure that the learned representations have better consistency between each class of view, we utilize encoder architecture without shared weights to extract local and global information. Specifically, for simplicity, we choose GCN (Kipf and Welling, 2016) as the basic encoder to model structural dependencies, and we feed all local semantic timespan views into the encoder f_l and all global semantic timespan views into encoder f_g . The node representations are updated by multi-layer graph convolution:

$$\mathbf{H}^l = f_l(\mathbf{A}, \mathbf{X}), \quad (8)$$

$$\mathbf{H}^g = f_g(\mathbf{S}, \mathbf{X}), \quad (9)$$

where $\mathbf{H}^l \in \mathbb{R}^{N \times d}$ and $\mathbf{H}^g \in \mathbb{R}^{N \times d}$ are the node representations learned from \mathbf{A} and \mathbf{S} , respectively. It is worth noting that the different views sampled on the dynamic graph according to the timespan view sampling layer contain different sets of nodes and edges. Therefore, we used the minibatch training approach in the specific implementation.

4.5. Projection Head Layer

The base encoder extracts the representation of nodes from the local and global timespan views. Then, we feed the representations containing local and global information respectively into a projection head, which maps the representation to the space where contrastive loss is applied. The projection head formula is as follows:

$$\mathbf{z}_{i,l}^{\mathcal{T}}, \mathbf{z}_{i,g}^{\mathcal{T}} = \text{proj}(\mathbf{h}_{i,l}^{\mathcal{T}}), \text{proj}(\mathbf{h}_{i,g}^{\mathcal{T}}), \quad (10)$$

where $\mathbf{h}_{i,l}^{\mathcal{T}}$ and $\mathbf{h}_{i,g}^{\mathcal{T}}$ are the local and global representations of node i extracted under the timespan view \mathcal{T} , respectively. $\text{proj}(\cdot)$ is composed of a fully connected layer, l_2 normalized and LeakyReLU activation function.

4.6. Contrastive Loss Function

Based on the observation that node labels tend to be invariant over the entire dynamic graph time period, we propose a new inductive bias on dynamic graphs, i.e., temporal translation invariance. Distinguishing from previous

work, we learn node embedding by maximizing the temporal consistency between local-local, local-global, and global-global semantic views. Specifically, in temporal translation invariance, we treat the semantics between locals or globals of the same/different node in different timespan views and the semantics between local and global of the same/different node in the same timespan view as positive/negative pairs. CLDG++ is trained to minimize temporal translation invariance. The contrastive learning loss of CLDG++ is defined as follows:

$$\mathcal{L} = \sum_{i=1}^N \sum_{q=1}^V \sum_{k \neq q}^V \left(\text{ctr} \left(\mathbf{z}_{i,l}^{\mathcal{T}_q}, \mathbf{z}_{i,l}^{\mathcal{T}_k} \right) + \text{ctr} \left(\mathbf{z}_{i,g}^{\mathcal{T}_q}, \mathbf{z}_{i,g}^{\mathcal{T}_k} \right) \right. \\ \left. + \text{ctr} \left(\mathbf{z}_{i,l}^{\mathcal{T}_q}, \mathbf{z}_{i,g}^{\mathcal{T}_q} \right) + \text{ctr} \left(\mathbf{z}_{i,l}^{\mathcal{T}_k}, \mathbf{z}_{i,g}^{\mathcal{T}_k} \right) \right) \quad (11)$$

where N is the batch size, and V is the multiple views sampled by the timespan view sampling layer. $\text{ctr}(\cdot, \cdot)$ is InfoNCE (Van den Oord et al., 2018) contrastive approach, which is defined in Eq. 12. CLDG exclusively focuses on local-local contrast, resulting in the loss of node i degenerates to $\text{ctr} \left(\mathbf{z}_{i,l}^{\mathcal{T}_q}, \mathbf{z}_{i,l}^{\mathcal{T}_k} \right)$.

$$\text{ctr} \left(\mathbf{z}_{i,\cdot}^{\mathcal{T}_q}, \mathbf{z}_{i,\cdot}^{\mathcal{T}_k} \right) = -\log \frac{\exp \left(\mathbf{z}_{i,\cdot}^{\mathcal{T}_q} \cdot \mathbf{z}_{i,\cdot}^{\mathcal{T}_k} / \tau \right)}{\sum_{j=1}^N \exp \left(\mathbf{z}_{i,\cdot}^{\mathcal{T}_q} \cdot \mathbf{z}_{j,\cdot}^{\mathcal{T}_k} / \tau \right)}, \quad (12)$$

where τ is a temperature parameter.

To sum up, in each training epoch, we first sample multiple different views through the timespan view sampling layer. Subsequently, a global diffusion timespan view is generated by employing PPR and heat kernel on the sampled local timespan views. Afterward, the local and global node representations in the minibatch are learned by using the encoder and projection head. Finally, the parameters in the encoder and projection head are updated by minimizing Eq. 11.

4.7. Anomaly Discriminator

CLDG and CLDG++ learn good node representation through temporal translation invariance. However, we realize that anomalous nodes may violate the assumption of temporal translation invariance. Instances such as an

anomalous company exhibiting a substantial deviation in traded goods from its established business scope over a period of time or experiencing a sudden surge in trading activities over a short period of time. Capturing such anomalies would make it possible to extend CLDG and CLDG++ to anomalous node detection. A new challenge is how to accurately quantify each node-specific anomaly score from the learned low-dimensional node features without a given anomalous node.

To address the above challenges, we design an anomaly discriminator in the inference phase. Specifically, after the model training is completed, the V timespan views are first sampled in the inference phase using the sequential sampling strategy. Then node i is encoded using the base encoder and the projection head, the learned representation of node i as $[\mathbf{z}_{i,l}^{\mathcal{T}_1}, \mathbf{z}_{i,l}^{\mathcal{T}_2}, \dots, \mathbf{z}_{i,l}^{\mathcal{T}_V}]$. Finally, given that anomalous nodes typically do not follow temporal translation invariance, we hypothesize that anomalous nodes have low context consistency of their representations between timespan views, while normal nodes tend to have high consistency of their representations between timespan views. Our anomaly discriminator computes the anomaly score by capturing the context consistency and stability between timespan views:

$$\overline{S}_i = \sum_{q=1}^V \sum_{k \neq q}^V D(\mathbf{z}_{i,l}^{\mathcal{T}_q}, \mathbf{z}_{i,l}^{\mathcal{T}_k}) / (V \cdot (V - 1)), \quad (13)$$

$$S(v_i) = \overline{S}_i + \sqrt{\sum_{q=1}^V \sum_{k \neq q}^V \left(D(\mathbf{z}_{i,l}^{\mathcal{T}_q}, \mathbf{z}_{i,l}^{\mathcal{T}_k}) - \overline{S}_i \right)^2 / (V \cdot (V - 1))}, \quad (14)$$

where $S(v_i)$ is the anomaly score of node i . The larger $S(\cdot)$ means a higher abnormality. $D(q, k) = 1 - q^\top k / \|q\| \|k\|$ is the consistency distance measure function. \overline{S}_i computes the context consistency between timespan views, while Eq. 14 computes the stability between contexts.

4.8. Complexity Analysis

Our proposed method is agnostic to the size of the graph, with its parameters primarily concentrated in the base encoder and projection head, rendering it inherently lightweight. The time complexity is $O(L|\mathcal{V}|d^2 + L|\mathcal{E}|d)$, where \mathcal{V} is the set of nodes, \mathcal{E} is the set of edges, L represents the number of layers of the graph convolution, and d is the node feature dimension.

This is significantly lower than existing dynamic graph representation learning methods that additionally consider sequential models. Furthermore, the space complexity of our method’s parameters is $O(Ld^2)$. However, existing dynamic graph representation learning methods typically integrate node and edge features into the model parameters, increasing the space complexity by $O(|\mathcal{V}|d + |\mathcal{E}|d)$. More importantly, this would result in parameter space and runtime increasing significantly with the scale of the graph, rendering it impractical for large-scale graphs.

4.9. Advantages over Dynamic Graph Methods

Compared with previous dynamic graph work, CLDG and CLDG++ have the following advantages:

Better Generality. Existing dynamic graph work is generally designed solely for discrete-time dynamic graphs or continuous-time dynamic graphs. However, the timespan view sampling layer enables CLDG and CLDG++ to handle both discrete-time and continuous-time dynamic graphs.

Better Scalability. The encoder module of CLDG and CLDG++ can use any network architecture, and any effective encoder in the future can also be integrated into CLDG and CLDG++ in a way similar to hot swap.

Lower Space and Time Complexity. A generalized dynamic graph learning paradigm is to use graph neural networks to model structural information, and then use sequential models to explicitly model evolutionary information. However, CLDG and CLDG++ implicitly exploit the additional temporal cues provided by dynamic graphs through contrastive learning, omitting the sequential model architecture. Therefore it has lower space and time complexity.

5. Experiments

In this section, we first introduce seven real-world dynamic graph datasets. Then, we conduct extensive experiments to prove the CLDG and CLDG++ yield consistent and significant improvements over baselines. Finally, ablation experiments on different components such as the timespan view sampling layer and base encoder layer. Meanwhile, the analysis of space and time complexity further proves the lightweight of our model. The code and data are publicly available ¹. The experiment aims to answer the following questions:

¹<https://github.com/yimingxu24/CLDG>

Table 2: Statistics of the Datasets.

# Dataset	# nodes	# temporal edges	# classes
DBLP	25,387	185,480	10
Bitcoinotc	5,881	35,592	3
TAX	27,097	315,478	12
BITotc	4,863	28,473	7
BITalpha	3,219	19,364	7
TAX51	132,524	467,279	51
Reddit	898,194	2,575,464	3

- **RQ₁**: Does our model yield state-of-the-art results for unsupervised dynamic graph representation learning in the node classification task?
- **RQ₂**: Does our model achieve state-of-the-art results on the anomaly detection tasks?
- **RQ₃**: How to choose the appropriate timespan as a contrastive view?
- **RQ₄**: Does our model allow various encoder architecture choices without any limitations? Do different encoders have any effect on CLDG and CLDG++?
- **RQ₅**: How about the time complexity and space complexity of our model?
- **RQ₆**: How do different contrast pairs affect CLDG++?
- **RQ₇**: How do various hyperparameters impact CLDG++ performance?

5.1. Experiment Preparation

5.1.1. Real-world Dataset

Seven datasets from four fields (i.e. academic citation network, tax transaction network, Bitcoin network, and Reddit hyperlink network) are used to evaluate the quality of representations learned by CLDG and CLDG++. The statistics of the seven datasets are shown in Table 2.

Academic Citation Network. The DBLP dataset is extracted from the DBLP ². The label is the research field of researchers. The label information divides researchers into ten different research areas, and each researcher has only one label.

²<http://dblp.uni-trier.de>

TAX Transaction Networks. The TAX and TAX51 company industry classification datasets are extracted from the tax transaction network data of two cities provided by the tax bureau. It consists of companies as vertices, and transaction relationships between companies as edges. The industry code of each company is provided by the tax bureau as labels of the dataset.

Bitcoin Networks. Bitcoin is a cryptocurrency used for anonymous transactions on the web. Due to the risk of trading with anonymity, this has led to the emergence of several exchanges where Bitcoin users rate how much they trust other users. Bitcoinotc, BITotc (Kumar et al., 2016; Liu and Liu, 2021) and BITalpha (Kumar et al., 2016; Liu and Liu, 2021) are three datasets from two bitcoin trading platforms, OTC and alpha ³. The label is the credit rating of the Bitcoin user.

Reddit Hyperlink Network. We construct the Reddit dataset from the Subreddit Hyperlink Network ⁴. It consists of posts and hyperlinks in the community as nodes. The source and link relationship between each hyperlink and the post as edges. Each hyperlink is annotated with the sentiment of the source community post towards the target community post. This dataset can be used for sentiment classification.

For the anomaly detection task, since the above datasets have no anomalies by default, we follow previous work (Ding et al., 2019b; Song et al., 2007) and inject a combined set of structural and attribute anomalies for each dataset. Specifically, for structural anomalies, we randomly select some nodes that may be initially unconnected, and add links with the same timestamps between them, making them a fully connected clique. The timestamp of each clique is randomly generated within the overall timespan of the graph. All nodes in such a clique are marked as structural anomalies because the nodes within the clique are much more closely connected to each other than the average, which can be regarded as a typical structural anomaly in the real world (Skillicorn, 2007; Liu et al., 2021a). Meanwhile, for attribute anomalies, we create feature anomalies by perturbing the node attributes of a timespan. When injecting a single node feature anomaly, we randomly pick a node v_i as the target node and sample another k nodes as the candidate set. We choose the node v_j with the largest Euclidean distance from the feature of node v_i among the k nodes. Then, we inject the feature of v_j into a certain

³<https://www.bitcoin-otc.com/> and <https://btc-alpha.com/>

⁴<http://snap.stanford.edu/data/soc-RedditHyperlinks.html>

timespan of v_i , while leaving the feature of v_i unchanged in other timespans. To ensure a sufficiently large disturbance amplitude, we set $k = 50$. Since the static graph method cannot handle temporal inputs, we introduce the average of all timespan node features to construct feature anomalies for the static graph method. Finally, we injected 600, 300, 600, 300, 300, 6000, and 6000 anomalies into 7 datasets respectively.

5.1.2. Evaluation Protocols

We divide the seven datasets according to the 1:1:8 split method of training set: validation set: test set. Semi-supervised methods train the model through training and validation sets, outputting predicted labels for each node in the test set. Our method and other unsupervised methods follow a linear evaluation scheme as introduced in (Velickovic et al., 2019), where each model is firstly trained in an unsupervised manner. After training, freeze the model parameters and output the learned representations for all nodes. Subsequently, the representation is fed into a linear classifier, noting that only the node embeddings in the training set are used to train the classifier. We report the Accuracy and Weighted-F1 metrics for node classification in the test set. For the anomaly detection task, we still measure our proposed framework and baselines based on the ROC-AUC (AUC for short), which is widely used to evaluate anomaly detection performance in previous work (Ding et al., 2019a; Peng et al., 2018).

5.1.3. Implementation Details

Adam optimizer (Kingma and Ba, 2014) is used in the training model stage and the training linear classifier stage. In the training model stage, the learning rate of the encoder and projection head is 4×10^{-3} , and the weight decay is 5×10^{-4} . In the training linear classifier stage, the learning rate is 10^{-2} , the weight decay is 10^{-4} . The base encoder adopts a two-layer GCN, the batch size is 256, the hidden layer dimension is 128, and the output dimension is 64. The random sampling strategy is chosen for the BITotc and TAX51 datasets, while the sequential sampling strategy is employed for the other datasets. The heat kernel is selected as the graph diffusion instance for the Bitcoinotc and TAX51 datasets, and others are PPR.

5.2. Node Classification (**RQ₁**)

To answer **RQ₁**, we compare CLDG and CLDG++ with 12 state-of-the-art algorithms on the seven dynamic graph datasets. The semi-supervised

Table 3: Experimental results (%) of classification tasks on seven datasets. We report both mean Accuracy and Weighted-F1, the input column highlights the data required for model training (\mathbf{X} is the node features, \mathbf{A} is the adjacency matrix, \mathbf{S} is the diffusion matrix, \mathbf{T} is the time information, and \mathbf{Y} is the node labels). Bold represents the optimal in the unsupervised method, and underlined represents the global optimal.

	Method	Input	DBLP		Bitcoinotc		TAX		BITotc		BITalpha		TAX51		Reddit	
			Acc	Wei	Acc	Wei	Acc	Wei	Acc	Wei	Acc	Wei	Acc	Wei	Acc	Wei
Supervised	LP	A, Y	52.18	51.54	41.97	31.25	35.67	30.88	60.24	50.28	76.97	67.18	28.82	24.36	66.71	60.88
	GCN	X, A, Y	71.35	71.08	54.61	54.41	71.65	71.37	59.24	50.52	76.19	73.65	40.42	33.64	67.83	63.26
	GAT	X, A, Y	70.01	69.21	52.46	50.60	62.00	59.78	62.59	48.34	80.21	71.40	38.82	30.21	69.31	58.01
	GraphSAGE	X, A, Y	72.36	71.99	57.29	56.30	64.36	63.73	62.68	<u>56.99</u>	79.89	<u>74.24</u>	40.80	<u>33.79</u>	71.37	<u>65.74</u>
Unsupervised	CAW	X, A, T	55.64	51.38	59.85	57.92	53.25	47.11	63.56	53.59	77.64	71.99	36.52	29.52	67.79	57.80
	TGAT	X, A, T	57.48	51.96	58.56	55.73	50.12	45.62	62.53	49.53	77.63	68.03	34.50	28.44	65.57	56.81
	DySAT	X, A, T	54.12	52.48	51.32	48.80	52.31	51.42	62.01	48.70	77.61	68.07	23.81	22.89	-	-
	MNCI	X, A, T	67.03	66.46	55.14	54.79	45.44	37.13	63.49	54.66	79.04	71.80	39.13	32.29	70.94	65.26
	DGI	X, A	69.97	69.40	56.67	55.34	66.57	65.87	61.68	51.65	78.56	73.19	39.20	31.61	70.58	60.95
	GRACE	X, A	71.27	70.71	54.50	53.48	67.43	66.79	62.49	48.06	77.60	67.81	-	-	-	-
	MVGRL	X, A, S	71.32	70.91	55.31	54.54	67.70	67.08	59.62	53.00	75.26	72.71	-	-	-	-
	CCA-SSG	X, A	68.28	67.60	56.48	54.83	67.62	67.14	63.47	51.70	79.97	72.69	37.04	29.69	69.46	58.69
	CLDG	X, A, T	71.80	71.55	59.17	58.45	69.62	69.18	<u>65.68</u>	54.74	80.61	72.90	40.44	32.36	71.69	62.87
	CLDG++	X, A, S, T	72.94	72.69	<u>59.88</u>	<u>58.96</u>	73.21	<u>73.01</u>	65.37	54.44	80.63	72.87	<u>41.05</u>	33.15	<u>71.73</u>	62.56

model in the baseline includes label propagation (LP), GCN, GAT, and GraphSAGE. We also compare with unsupervised dynamic graph models including CAW, TGAT, DySAT, and MNCI, and unsupervised contrastive learning methods including DGI, GRACE, MVGRL, and CCA-SSG. We use the Accuracy and Weighted-F1 as the evaluation metrics, bold indicates that the method is optimal among unsupervised methods, and underlined indicates that it is optimal among all baselines. We report classification results on seven datasets in Table 3.

We can observe that both CLDG and CLDG++ outperform other unsupervised methods. Among the Accuracy and Weighted-F1 metrics of the seven datasets, 12 metrics are optimal among the unsupervised methods. CLDG outperforms the previous state-of-the-art GraphSAGE model by 1.47% on the average of all metrics. CLDG++, which introduces local-global and global-global contrasts, outperforms CLDG in 10 metrics, which indicates that retaining more information helps learn high-quality node representations. Supervised methods are overall very competitive. In contrast, LP limits expressive power by ignoring the node feature matrix \mathbf{X} . However, without label supervision, our method even shows superior results than all supervised models in 10 metrics. This proves that using the local-local and

Table 4: AUC Scores (%) for Anomaly Detection on seven datasets (OOM: CPU/CUDA Out of Memory). Bold represents the global optimal.

Method	DBLP	Bitcoinotc	TAX	BITotc	BITalpha	TAX51	Reddit
AEGIS	59.18 \pm 3.17	50.97 \pm 6.15	59.62 \pm 4.06	53.17 \pm 0.57	54.13 \pm 4.57	54.52 \pm 1.67	OOM
CoLA	71.06 \pm 0.24	79.44 \pm 1.46	66.68 \pm 0.24	81.80 \pm 0.31	77.65 \pm 0.19	77.29 \pm 0.12	OOM
ANEMONE	70.69 \pm 1.00	79.28 \pm 0.56	67.46 \pm 1.29	80.09 \pm 0.93	72.70 \pm 1.47	76.61 \pm 0.23	OOM
GRADATE	69.53 \pm 0.10	74.14 \pm 0.32	70.62 \pm 0.49	73.12 \pm 0.42	68.64 \pm 0.43	OOM	OOM
NetWalk	54.42 \pm 0.33	56.13 \pm 0.71	55.42 \pm 0.64	58.46 \pm 0.44	64.12 \pm 0.60	OOM	OOM
TADDY	50.93 \pm 0.59	50.58 \pm 0.33	50.83 \pm 0.55	51.48 \pm 0.38	50.42 \pm 0.30	OOM	OOM
SAD	78.24 \pm 0.31	75.67 \pm 0.28	70.61 \pm 0.52	71.29 \pm 0.46	71.83 \pm 0.45	61.70 \pm 0.79	72.19 \pm 0.60
CLDG	84.89 \pm 0.24	80.21 \pm 0.99	71.81 \pm 0.15	81.55 \pm 0.84	77.70 \pm 0.99	79.51 \pm 0.13	71.53 \pm 0.28
CLDG ++	86.41 \pm 0.32	81.97 \pm 1.08	72.86 \pm 0.28	82.92 \pm 0.54	79.71 \pm 0.36	81.02 \pm 0.26	72.77 \pm 0.08

global-global contrasts in different timespan views, as well as the local-global contrast in the same timespan view in dynamic graphs, provides rich graph information and is sufficient for classification tasks.

In summary, experimental results demonstrate that CLDG++ generalizes contrastive learning from static graphs to dynamic graphs through multi-scale temporal translation invariance on graphs, and implicitly utilizes temporal information to achieve state-of-the-art results.

5.3. Anomaly Detection (**RQ₂**)

To address **RQ₂**, we compare our model with seven popular graph-based anomaly detection methods chosen as baselines. The unsupervised models in the baselines include AEGIS, ANEMONE, CoLA, GRADATE, NetWalk, and TADDY. SAD represents a semi-supervised anomaly detection approach. Among the baselines, models NetWalk, TADDY, and SAD incorporate temporal information in their methods. NetWalk and TADDY primarily focus on edge anomaly detection. Therefore, after training the models, we preserve the learned node representations and uniformly input them into our proposed anomaly discriminator to compute node anomaly scores. Table 4 reports the anomaly detection performance of all methods on 7 datasets. First, CLDG outperforms all unsupervised baselines, while CLDG++ surpasses all baselines, which strongly proves the success of CLDG and its extended version in the anomaly detection task. Second, we can observe that the three contrastive learning-based baselines CoLA, ANEMONE and GRADATE are all very competitive, indicating that contrastive learning is generally effective on anomaly detection tasks. Third, one possible reason for the mediocre

performance of NetWalk and TADDY on several datasets is that they were originally designed to detect abnormal edges. SAD is specifically designed to detect node anomalies while using a semi-supervised training paradigm to achieve better performance. Finally, the above baselines typically require complete adjacency and attribute matrices as input, making them impractical for large-scale graph data due to the explosive memory requirements.

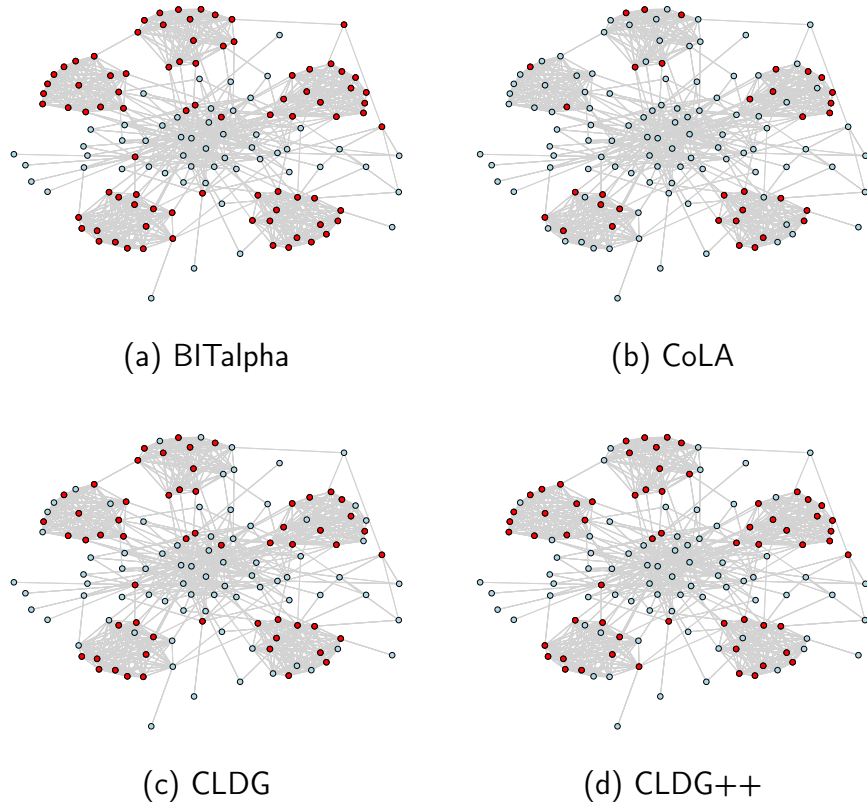


Figure 6: Visualization of detection results on BITalpha dataset. Abnormal/normal nodes or nodes detected as abnormal/normal by the model are marked in red/blue. (a) is the ground truth of the sampled BITalpha dataset, and the others are the anomaly detection results of CoLA, CLDG, and CLDG++ respectively.

In addition to the aforementioned quantitative analysis, we also present qualitative visual case studies. Figure 6a illustrates a sampled subgraph from BITalpha, where the ground truth anomalies and normal nodes are denoted by red and blue colors, respectively. In CoLA, CLDG, and CLDG++, we

Table 5: Comparison of different timespan view sampling architectures, sampling strategy, sampling view timespan size s and number of sampling views v in the DBLP and TAX dataset. The sampling strategy with a low overlap rate between views, such as sequential and random, and sampling more views are beneficial to CLDG, and the timespan of sampling views is robust to CLDG.

$v \backslash s$	Sequential			High Overlap Rate			Low Overlap Rate			Random		
	6	8	10	6	8	10	6	8	10	6	8	10
2	71.11	71.01	70.84	69.44	68.92	69.16	70.26	70.59	70.10	71.01	70.69	70.48
3	71.34	71.10	71.17	69.92	69.78	69.56	70.85	70.73	70.79	70.95	71.06	70.75
4	71.40	71.34	71.00	70.01	69.75	69.82	70.80	70.60	70.73	70.53	71.06	70.61
5	71.55	71.49	71.23	70.48	70.62	70.23	71.16	70.96	70.54	71.04	70.77	70.74

(a) Dataset: **DBLP**, base encoder: **GCN**, epoch: **200**.

$v \backslash s$	Sequential			High Overlap Rate			Low Overlap Rate			Random		
	6	8	10	6	8	10	6	8	10	6	8	10
2	67.05	67.94	65.75	63.52	62.87	62.68	64.98	64.22	63.51	65.26	65.13	65.08
3	67.65	67.25	66.58	63.79	63.68	63.04	64.53	64.76	63.91	66.33	65.57	65.63
4	68.99	67.85	67.51	64.22	63.69	63.40	64.91	64.53	64.05	66.80	66.46	65.97
5	68.98	67.01	67.60	64.26	63.35	63.50	65.03	64.76	64.11	66.79	66.18	66.19

(b) Dataset: **TAX**, base encoder: **GCN**, epoch: **200**.

mark the 300 nodes in the dataset with the highest node anomaly scores in red. As shown in Figure 6b, such as the clique located in the upper-left corner, most of the structural anomalous nodes are misclassified as normal nodes by CoLA. The observations from Figure 6c and Figure 6d reveal that our model accurately detects the majority of abnormal nodes, including structural abnormalities in various clusters. Moreover, CLDG++ exhibits higher detection accuracy compared to CLDG. This finding underscores the strong anomaly detection performance of both CLDG and its extended version, aligning with the results presented in Table 4.

5.4. View Sampling Architecture (RQ₃)

The timespan view sampling module consists of three factors: sampling strategy, view timespan factor s and the number of views sampled v . We design four different sampling strategies, sequential, high overlap rate, low overlap rate and random, and the details of the sampling strategy are demon-

strated in this section 4.2. v controls the number of the sampling timespan views, and s controls the timespan size of the view. We show in Table 5a and Table 5b how the three factors jointly affect the performance of CLDG on the DBLP and TAX datasets.

The variation on the dynamic graph is continuous and smooth, and if the timespan views overlap physically, better results may be achieved by sharing more similar semantic contexts. Therefore, the main difference between the four sampling strategies is the overlap rate between views. However, the better performers of the four strategies are sequential and random. The high overlap rate strategy tends to be the worst performer, on average 1.41% and 4.01% lower than the sequential strategy in the DBLP and TAX datasets, respectively. This is a very interesting phenomenon, illustrating that on a dynamic graph with temporal translation invariance, a high overlap rate may lead to an overly simplistic contrastive learning task, thereby compromising the robustness of the model. The sequential and randomized approaches maintain high-level semantic consistency rather than just low-level physical consistency allowing for better performance on the test set. The view timespan factor s , i.e., constructed views with different timespans, is relatively robust in both datasets and seems to have little effect on CLDG. In practice, we can choose some timespans with physical significance, such as day, week, month, and so on. Finally, on the number of timespan views v , we find that $v = 3, 4, 5$ on average 0.37%, 0.34%, 0.60%, and 0.40%, 0.87%, 0.82% higher than $v = 2$, in DBLP and TAX datasets, respectively. This indicates that more timespan views are beneficial for CLDG, but the average improvement is smaller after the number of views exceeds 3.

In general, the sampling strategy with the low overlap rate between views and sampling more views is beneficial to CLDG, and the timespan of constructed views is robust.

5.5. Encoder Architecture (**RQ₄**)

To answer **RQ₄**, we implement three classical GNN encoders (GCN, GAT and GraphSAGE) for CLDG and CLDG++. We conduct experiments on the DBLP, BITalpha, and TAX51 datasets. The number of layers of the encoder is 2, the timespan view sampling strategy is sequential, s is 4, v is 2, the epoch is 200, 100 and 200, respectively. Table 6 shows the classification results of different encoder architectures in the test set. The experimental results show that all three encoders have very competitive performance. Under the current parameter settings, GraphSAGE performs best in CLDG,

Table 6: Scalability verification of CLDG and CLDG++ by comparing the results of different encoder variants on three datasets.

Encoder		DBLP		BITalpha		TAX51	
		Acc	Wei-F1	Acc	Wei-F1	Acc	Wei-F1
CLDG	GCN	71.48	71.18	80.14	72.18	40.07	32.02
	GAT	73.49	73.16	80.12	71.79	41.64	32.85
	GraphSAGE	73.19	72.51	80.09	71.97	41.34	34.78
CLDG++	GCN	72.98	72.72	80.14	72.27	40.68	32.58
	GAT	74.47	74.24	80.21	71.93	42.96	34.51
	GraphSAGE	73.71	73.06	80.19	71.68	43.80	34.85

averaging 1.14% higher than CLDG with the GCN encoder on the three datasets. In CLDG++, GAT is the best encoder choice, 1.16% higher than GCN. Meanwhile, we can observe that CLDG++, which considers global information, shows better performance compared to CLDG in various encoder selections, improving by 0.72%, 0.88%, and 0.57% in GCN, GAT, and GraphSAGE respectively.

In conclusion, our experiments illustrate that CLDG and CLDG++ exhibit flexibility in choosing various encoder architectures without any limitations. Notably, all employed encoders consistently achieve highly competitive results, showcasing the remarkable robustness of CLDG and CLDG++.

5.6. Space and Time Complexity Analysis (RQ₅)

To answer RQ₅, we compared CLDG and CLDG++ with four other dynamic graph methods (CAW, TGAT, DySAT, and MNCI) in terms of space and time complexity. In Table 7, we measure the space and time complexity by the number of parameters and the model training time, respectively. In terms of space complexity, first, the parameters of our model do not increase with the increase in graph size. However, other dynamic graph models have a maximum of 104.21, 123.54, 1.00, and 265.39 times increase in parameters on the seven datasets, respectively. The CLDG and CLDG++ parameters are derived from the base encoder and the projection head, and the base encoder can also be replaced with an encoder of lower space complexity and time complexity in the future. Then, the parameters of CLDG are much smaller than the existing SOTA dynamic graph model. The parameters of CAW, TGAT, DySAT, and MNCI are 17,840.6, 17,813.8, 2.0, and 5,785.4 times of

Table 7: Comparison of space and time complexity of dynamic graph method on seven datasets. CLDG has lower space and time complexity.

Method	DBLP		Bitcoinotc		TAX		BITotc		BITalpha		TAX51		Reddit	
	Param	Time	Param	Time	Param	Time	Param	Time	Param	Time	Param	Time	Param	Time
CAW	56.76M	9403s	13.39M	3498s	90.47M	30702s	11.31M	2510s	8.56M	1768s	156.32M	329336s	892.03M	361580s
TGAT	55.41M	5607s	12.05M	669s	89.13M	6067s	9.96M	1713s	7.21M	642s	154.98M	55066s	890.69M	50441s
DySAT	0.10M	5103s	0.10M	513s	0.10M	5781s	0.10M	422s	0.10M	456s	0.10M	46173s	0.10M	-
MNCI	8.22M	4308s	1.94M	745s	8.78M	7580s	1.62M	550s	1.09M	481s	42.72M	10463s	289.27M	46586s
CLDG	0.05M	297s	0.05M	136s	0.05M	312s	0.05M	74s	0.05M	248s	0.05M	348s	0.05M	551s
CLDG++	0.06M	3989s	0.06M	280s	0.06M	923s	0.06M	257s	0.06M	389s	0.06M	1728s	0.06M	3865s

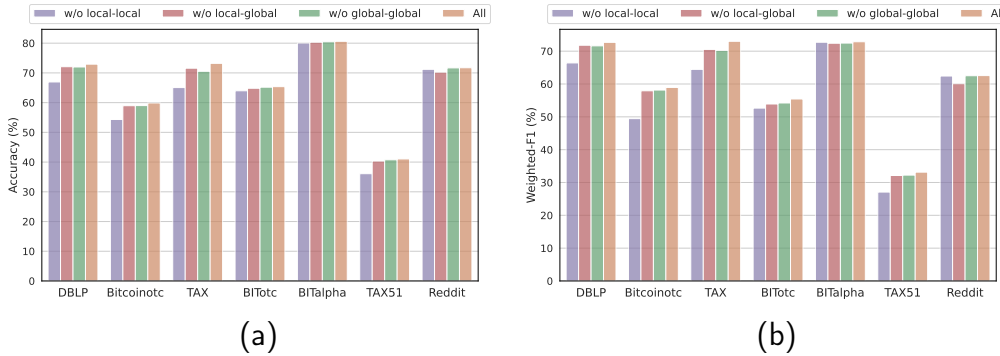


Figure 7: Ablation study on different variants.

CLDG on the Reddit dataset, respectively. Finally, in terms of time complexity, CLDG is implemented with a graph neighbor sampler, and the running time of CLDG is 946.4, 158.2, 132.7, and 30.1 times faster than CAW, TGAT, DySAT, and MNCI on TAX51 dataset. Due to the graph diffusion performed on the adjacency matrix of each sampled timespan view in CLDG++, the running time of the method increases. However, we still observe that the running time of CLDG++ remains significantly lower compared to existing dynamic graph representation learning methods.

In conclusion, CLDG and CLDG++ have lower space and time complexity than existing dynamic graph methods, and are more significant on larger-scale graphs. It is proved that our method is easier to generalize to larger-scale graph learning.

5.7. Ablation Study (RQ₆)

To validate the effectiveness of each contrast pair in CLDG++, we analyze the impact of local-local contrast loss, local-global contrast loss, and

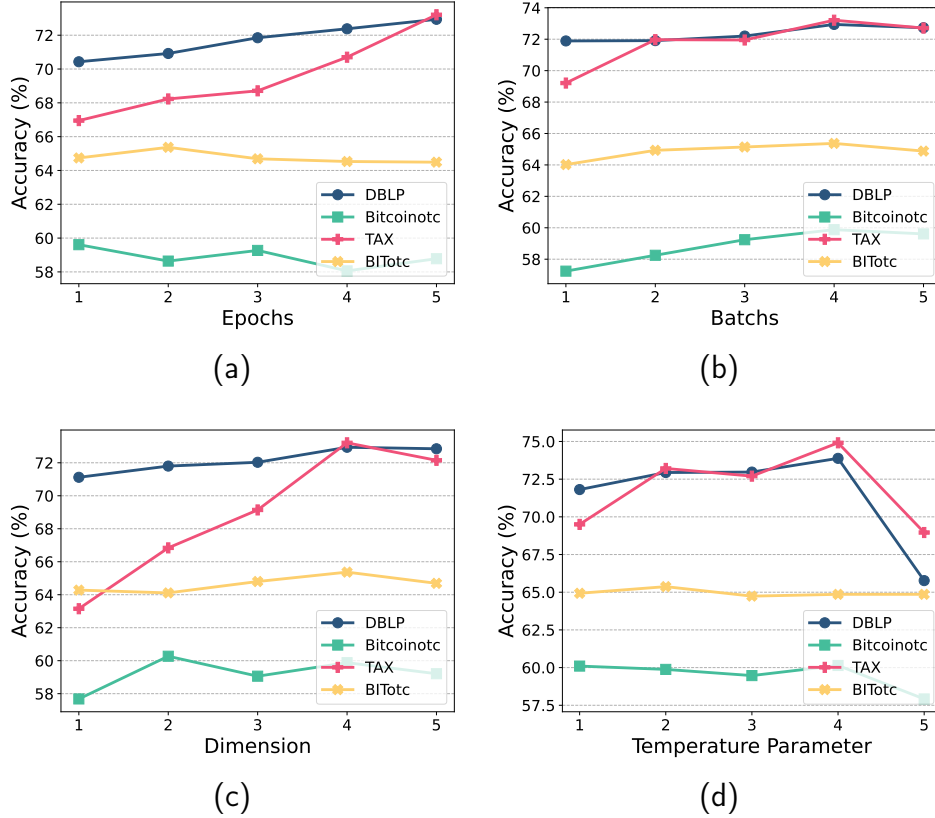


Figure 8: Parameter sensitivity of CLDG++. Effect of (a) epoch, (b) batch size, (c) hidden layer dimension, and (d) temperature parameter on the node classification.

global-global contrast loss within our method. "W/o" denotes the removal of the loss during training. The results of our ablation study on 7 datasets are presented in Figure 7. It is evident that CLDG++ consistently outperforms other variants regarding overall performance. Specifically, the absence of local-local contrast, local-global contrast, and global-global contrast leads to performance degradation by 3.88%, 0.92% and 0.74% in accuracy (%), and 4.78%, 1.41% and 1.03% in weighted-F1 (%), respectively. This observation provides evidence that the local-local contrast plays a dominant role in representation learning. In summary, the performance degradation observed when any loss function is absent in CLDG++ highlights the importance of each contrast pair.

5.8. Hyperparameters Sensitivity (RQ₇)

We investigate the sensitivity of the parameters and report the Accuracy (%) results for four datasets with various parameters in Figure 8.

Effect of epoch. We initially investigate the effect of epochs on the performance of CLDG++. The results, depicted in Fig. 8a, demonstrate that the performance of the DBLP and TAX datasets steadily improves as the number of epochs increases. Conversely, the Bitcoinotc and BITotc datasets exhibit minimal variance in performance as the number of epochs grows. This discrepancy can be attributed to the fact that larger datasets necessitate a greater number of epochs for training, whereas smaller datasets require fewer epochs to converge to the optimal solution.

Effect of batch size. We then examine the effect of batch size on the performance of CLDG++. The corresponding results are presented in Fig. 8b. Across all four datasets, we observe a general improvement in classification performance as the batch size increases. However, when the batch size is 512, performance degradation is observed on some datasets. One possible reason is that a larger batch size causes more nodes with the same label to be pulled apart in the Euclidean space. Adjusting appropriate temperature parameters τ may alleviate this problem.

Effect of hidden layer dimension. We explore the impact of output dimension on CLDG++. The results are shown in Fig. 8c. Notably, on the DBLP and TAX datasets, we observe an improvement in classification performance as the output dimensionality increases. However, on the Bitcoinotc and BITotc datasets, the classification performance initially improves but eventually diminishes with increasing output dimension. The reason is that larger hidden layer dimensions may introduce additional redundancy on smaller datasets.

Effect of temperature parameter. We investigate the effect of varying the value of the temperature parameter τ in Eq. 12, which is often used to control the sharpness of the similarity scores or logits produced by the contrastive loss function. When the temperature coefficient is large, the similarity between samples becomes more difficult to distinguish. Specifically, on DBLP, Bitcoinotc, and TAX datasets, setting $\tau = 0.5$ significantly reduces the model’s accuracy and generalization ability. Conversely, when the temperature coefficient is small, excessive attention to marginal similarity differences can also lead to a performance decline.

6. Conclusions

To address the limitations of supervision and the disregard for temporal signals in graphs, we introduce a novel assumption known as temporal translation invariance. This assumption allows us to extend the unsupervised paradigm to dynamic graphs, enabling a more comprehensive understanding of the underlying patterns in the data. Specifically, we proposed a sampling layer to extract the temporally-persistent signals. Then, CLDG encourages the node to maintain consistent local representations, i.e., temporal translation invariance under the timespan views. In addition, we also propose its variant CLDG++, which reveals the global context through diffusion matrices and utilizes three different views, local-local, local-global, and global-global, to compose multi-scale contrastive learning objectives to mine rich feature, structural, and temporal information in dynamic graphs. Finally, we introduce a new unsupervised anomaly detection framework that applies the concept of temporal translation invariance to dynamic graph anomaly detection tasks. The experiments demonstrate that CLDG and CLDG++ are superior state-of-the-art unsupervised methods and are competitive with supervised methods in node classification and anomaly detection tasks. Future work will focus on lightweight explicit modeling and capturing the evolutionary information in the graph to delve deeper into the rich information inherent in the dynamic graph.

Acknowledgment

This research was partially supported by the National Natural Science Foundation of China, No. (62050194, 62002282, 62192781, 61721002 and 62302380), the China Postdoctoral Science Foundation No. (2020M683492, 2023M742789), the MOE Innovation Research Team No. (IRT_17R86), Project of XJTU Undergraduate Teaching Reform No. (20JX04Y), and Project of XJTU-SERVYOU Joint Tax-AI Lab.

References

- Baldi, P., 2012. Autoencoders, unsupervised learning, and deep architectures, in: Proceedings of ICML workshop on unsupervised and transfer learning, JMLR Workshop and Conference Proceedings. pp. 37–49.

- Breiger, R.L., Pattison, P.E., 1986. Cumulated social roles: The duality of persons and their algebras. *Social networks* 8, 215–256.
- Cappart, Q., Chételat, D., Khalil, E., Lodi, A., Morris, C., Veličković, P., 2021. Combinatorial optimization and reasoning with graph neural networks. *arXiv preprint arXiv:2102.09544* .
- Chen, T., Kornblith, S., Norouzi, M., Hinton, G., 2020. A simple framework for contrastive learning of visual representations, in: *ICML*, PMLR. pp. 1597–1607.
- Chien, E., Chang, W.C., Hsieh, C.J., Yu, H.F., Zhang, J., Milenkovic, O., Dhillon, I.S., 2021. Node feature extraction by self-supervised multi-scale neighborhood prediction. *arXiv preprint arXiv:2111.00064* .
- Cho, K., Van Merriënboer, B., Gulcehre, C., Bahdanau, D., Bougares, F., Schwenk, H., Bengio, Y., 2014. Learning phrase representations using rnn encoder-decoder for statistical machine translation. *arXiv preprint arXiv:1406.1078* .
- Davis, A., Gardner, B.B., Gardner, M.R., 1941. Deep south. the u.
- Derrow-Pinion, A., She, J., Wong, D., Lange, O., Hester, T., Perez, L., Nunkesser, M., Lee, S., Guo, X., Wiltshire, B., et al., 2021. Eta prediction with graph neural networks in google maps, in: *CIKM*, pp. 3767–3776.
- Ding, K., Li, J., Agarwal, N., Liu, H., 2021. Inductive anomaly detection on attributed networks, in: *Proceedings of the twenty-ninth international conference on international joint conferences on artificial intelligence*, pp. 1288–1294.
- Ding, K., Li, J., Bhanushali, R., Liu, H., 2019a. Deep anomaly detection on attributed networks, in: *SDM*, SIAM. pp. 594–602.
- Ding, K., Li, J., Liu, H., 2019b. Interactive anomaly detection on attributed networks, in: *Proceedings of the twelfth ACM international conference on web search and data mining*, pp. 357–365.
- Dornaika, F., Bi, J., Zhang, C., 2023. A unified deep semi-supervised graph learning scheme based on nodes re-weighting and manifold regularization. *Neural Networks* 158, 188–196.

- Dou, Y., Liu, Z., Sun, L., Deng, Y., Peng, H., Yu, P.S., 2020. Enhancing graph neural network-based fraud detectors against camouflaged fraudsters, in: Proceedings of the 29th ACM international conference on information & knowledge management, pp. 315–324.
- Duan, J., Wang, S., Zhang, P., Zhu, E., Hu, J., Jin, H., Liu, Y., Dong, Z., 2023. Graph anomaly detection via multi-scale contrastive learning networks with augmented view, in: AAAI, pp. 7459–7467.
- Fan, J., Weng, W., Tian, H., Wu, H., Zhu, F., Wu, J., 2024. Rgdan: A random graph diffusion attention network for traffic prediction. *Neural networks* 172, 106093.
- Feng, W., Zhang, J., Dong, Y., Han, Y., Luan, H., Xu, Q., Yang, Q., Kharlamov, E., Tang, J., 2020. Graph random neural networks for semi-supervised learning on graphs. *NeurIPS* 33, 22092–22103.
- Gao, T., Yao, X., Chen, D., 2021. Simcse: Simple contrastive learning of sentence embeddings. *arXiv preprint arXiv:2104.08821* .
- Gasteiger, J., Weissenberger, S., Günnemann, S., 2019. Diffusion improves graph learning. *NeurIPS* 32.
- Goyal, P., Chhetri, S.R., Canedo, A., 2020. dyngraph2vec: Capturing network dynamics using dynamic graph representation learning. *Knowledge-Based Systems* 187, 104816.
- Goyal, P., Kamra, N., He, X., Liu, Y., 2018. Dyngem: Deep embedding method for dynamic graphs. *arXiv preprint arXiv:1805.11273* .
- Grill, J.B., Strub, F., Altché, F., Tallec, C., Richemond, P., Buchatskaya, E., Doersch, C., Avila Pires, B., Guo, Z., Gheshlaghi Azar, M., et al., 2020. Bootstrap your own latent—a new approach to self-supervised learning. *NeurIPS* 33, 21271–21284.
- Han, B., Wei, Y., Wang, Q., Wan, S., 2023. Dual adaptive learning multi-task multi-view for graph network representation learning. *Neural Networks* 162, 297–308.
- Hassani, K., Khasahmadi, A.H., 2020. Contrastive multi-view representation learning on graphs, in: ICML, PMLR. pp. 4116–4126.

- He, K., Fan, H., Wu, Y., Xie, S., Girshick, R., 2020. Momentum contrast for unsupervised visual representation learning, in: CVPR, pp. 9729–9738.
- Hjelm, R.D., Fedorov, A., Lavoie-Marchildon, S., Grewal, K., Bachman, P., Trischler, A., Bengio, Y., 2018. Learning deep representations by mutual information estimation and maximization. arXiv preprint arXiv:1808.06670 .
- Hochreiter, S., Schmidhuber, J., 1997. Long short-term memory. *Neural computation* 9, 1735–1780.
- Jiang, B., Chen, Y., Wang, B., Xu, H., Luo, B., 2023. Dropagg: Robust graph neural networks via drop aggregation. *Neural Networks* 163, 65–74.
- Jin, M., Liu, Y., Zheng, Y., Chi, L., Li, Y.F., Pan, S., 2021. Anemone: Graph anomaly detection with multi-scale contrastive learning, in: CIKM, pp. 3122–3126.
- Kazemi, S.M., Goel, R., Jain, K., Kobzyev, I., Sethi, A., Forsyth, P., Poupart, P., 2020. Representation learning for dynamic graphs: A survey. *J. Mach. Learn. Res.* 21, 1–73.
- Kingma, D.P., Ba, J., 2014. Adam: A method for stochastic optimization. arXiv preprint arXiv:1412.6980 .
- Kipf, T.N., Welling, M., 2016. Semi-supervised classification with graph convolutional networks. arXiv preprint arXiv:1609.02907 .
- Kondor, R.I., Lafferty, J., 2002. Diffusion kernels on graphs and other discrete structures, in: ICML, pp. 315–22.
- Kumar, S., Spezzano, F., Subrahmanian, V., Faloutsos, C., 2016. Edge weight prediction in weighted signed networks, in: ICDM, IEEE. pp. 221–230.
- Kumar, S., Zhang, X., Leskovec, J., 2019. Predicting dynamic embedding trajectory in temporal interaction networks, in: SIGKDD, pp. 1269–1278.
- Li, Z., Chen, Q., Koltun, V., 2018. Combinatorial optimization with graph convolutional networks and guided tree search. *NeurIPS* 31.

- Liu, M., Liu, Y., 2021. Inductive representation learning in temporal networks via mining neighborhood and community influences, in: Proceedings of the 44th International ACM SIGIR Conference on Research and Development in Information Retrieval, pp. 2202–2206.
- Liu, Y., Li, Z., Pan, S., Gong, C., Zhou, C., Karypis, G., 2021a. Anomaly detection on attributed networks via contrastive self-supervised learning. *TNNLS* 33, 2378–2392.
- Liu, Y., Pan, S., Wang, Y.G., Xiong, F., Wang, L., Chen, Q., Lee, V.C., 2021b. Anomaly detection in dynamic graphs via transformer. *TKDE* .
- Lu, Y., Wang, X., Shi, C., Yu, P.S., Ye, Y., 2019. Temporal network embedding with micro-and macro-dynamics, in: *CIKM*, pp. 469–478.
- Ma, T., Shi, B., Xu, Y., Zhao, Z., Liang, S., Dong, B., 2023. Dygl: A unified benchmark and library for dynamic graph, in: Asia-Pacific Web (APWeb) and Web-Age Information Management (WAIM) Joint International Conference on Web and Big Data, Springer. pp. 389–401.
- Ma, X., Wu, J., Xue, S., Yang, J., Zhou, C., Sheng, Q.Z., Xiong, H., Akoglu, L., 2021. A comprehensive survey on graph anomaly detection with deep learning. *TKDE* .
- McCulloch, W.S., Pitts, W., 1943. A logical calculus of the ideas immanent in nervous activity. *The bulletin of mathematical biophysics* 5, 115–133.
- Van den Oord, A., Li, Y., Vinyals, O., 2018. Representation learning with contrastive predictive coding. *arXiv e-prints* , arXiv–1807.
- Page, L., Brin, S., Motwani, R., Winograd, T., 1999. The pagerank citation ranking: Bringing order to the web. Technical Report. Stanford InfoLab.
- Pareja, A., Domeniconi, G., Chen, J., Ma, T., Suzumura, T., Kanezashi, H., Kaler, T., Schardl, T., Leiserson, C., 2020. Evolvegcnn: Evolving graph convolutional networks for dynamic graphs, in: *AAAI*, pp. 5363–5370.
- Peng, Z., Luo, M., Li, J., Liu, H., Zheng, Q., et al., 2018. Anomalous: A joint modeling approach for anomaly detection on attributed networks., in: *IJCAI*, pp. 3513–3519.

- Sankar, A., Wu, Y., Gou, L., Zhang, W., Yang, H., 2020. Dysat: Deep neural representation learning on dynamic graphs via self-attention networks, in: WSDM, pp. 519–527.
- Shi, B., Dong, B., Xu, Y., Wang, J., Wang, Y., Zheng, Q., 2023. An edge feature aware heterogeneous graph neural network model to support tax evasion detection. *Expert Systems with Applications* 213, 118903.
- Skillicorn, D.B., 2007. Detecting anomalies in graphs, in: 2007 IEEE Intelligence and Security Informatics, IEEE. pp. 209–216.
- Song, L., Li, H., Tan, Y., Li, Z., Shang, X., 2024. Enhancing enterprise credit risk assessment with cascaded multi-level graph representation learning. *Neural Networks* 169, 475–484.
- Song, X., Wu, M., Jermaine, C., Ranka, S., 2007. Conditional anomaly detection. *TKDE* 19, 631–645.
- Tian, S., Dong, J., Li, J., Zhao, W., Xu, X., Song, B., Meng, C., Zhang, T., Chen, L., et al., 2023. Sad: Semi-supervised anomaly detection on dynamic graphs. *IJCAI* .
- Trivedi, R., Farajtabar, M., Biswal, P., Zha, H., 2019. Dyrep: Learning representations over dynamic graphs, in: *ICLR*.
- Veličković, P., Cucurull, G., Casanova, A., Romero, A., Lio, P., Bengio, Y., 2017. Graph attention networks. *arXiv preprint arXiv:1710.10903* .
- Velickovic, P., Fedus, W., Hamilton, W.L., Liò, P., Bengio, Y., Hjelm, R.D., 2019. Deep graph infomax. *ICLR (Poster)* 2, 4.
- Wang, D., Zhang, Z., Zhou, J., Cui, P., Fang, J., Jia, Q., Fang, Y., Qi, Y., 2021. Temporal-aware graph neural network for credit risk prediction, in: *SDM, SIAM*. pp. 702–710.
- Wang, H., Zhou, C., Chen, X., Wu, J., Pan, S., Wang, J., 2020. Graph stochastic neural networks for semi-supervised learning. *NeurIPS* 33, 19839–19848.
- Wu, S., Sun, F., Zhang, W., Xie, X., Cui, B., 2020. Graph neural networks in recommender systems: a survey. *ACM Computing Surveys (CSUR)* .

- Wu, Z., Xiong, Y., Yu, S.X., Lin, D., 2018. Unsupervised feature learning via non-parametric instance discrimination, in: CVPR, pp. 3733–3742.
- Xia, J., Wu, L., Chen, J., Hu, B., Li, S.Z., 2022. Simgrace: A simple framework for graph contrastive learning without data augmentation, in: WWW, pp. 1070–1079.
- Xu, D., Cheng, W., Luo, D., Liu, X., Zhang, X., 2019. Spatio-temporal attentive rnn for node classification in temporal attributed graphs., in: IJCAI, pp. 3947–3953.
- Xu, D., Ruan, C., Korpeoglu, E., Kumar, S., Achan, K., 2020. Inductive representation learning on temporal graphs. arXiv preprint arXiv:2002.07962 .
- Xu, Y., Chen, J., Peng, Z., Chen, Z., Lin, Q., Ma, L., Shi, B., Dong, B., 2025a. Court of llms: Evidence-augmented generation via multi-llm collaboration for text-attributed graph anomaly detection, in: Proceedings of the 33rd ACM International Conference on Multimedia, pp. 2437–2446.
- Xu, Y., Hua, X., Peng, Z., Shi, B., Chen, J., Fu, X., Wang, S., Dong, B., 2025b. Text-attributed graph anomaly detection via multi-scale cross-and uni-modal contrastive learning. ECAI .
- Xu, Y., Peng, Z., Shi, B., Hua, X., Dong, B., Wang, S., Chen, C., 2025c. Revisiting graph contrastive learning on anomaly detection: A structural imbalance perspective, in: Proceedings of the AAAI Conference on Artificial Intelligence, pp. 12972–12980.
- Xu, Y., Shi, B., Dong, B., Wang, J., Wei, H., Zheng, Q., 2025d. Ted: related party transaction guided tax evasion detection on heterogeneous graph. Data Mining and Knowledge Discovery 39, 15.
- Xu, Y., Shi, B., Ma, T., Dong, B., Zhou, H., Zheng, Q., 2023. Cldg: Contrastive learning on dynamic graphs, in: ICDE, IEEE. pp. 696–707.
- Xu, Y., Shi, B., Peng, Z., Liu, H., Dong, B., Chen, C., 2025e. Out-of-distribution generalization on graphs via progressive inference, in: Proceedings of the AAAI Conference on Artificial Intelligence, pp. 12963–12971.

- Xue, G., Zhong, M., Li, J., Chen, J., Zhai, C., Kong, R., 2022. Dynamic network embedding survey. *Neurocomputing* 472, 212–223.
- Xue, H., Yang, L., Jiang, W., Wei, Y., Hu, Y., Lin, Y., 2020. Modeling dynamic heterogeneous network for link prediction using hierarchical attention with temporal rnn, in: *ECML PKDD*, Springer. pp. 282–298.
- You, Y., Chen, T., Sui, Y., Chen, T., Wang, Z., Shen, Y., 2020. Graph contrastive learning with augmentations. *NeurIPS* 33, 5812–5823.
- Yu, W., Cheng, W., Aggarwal, C.C., Zhang, K., Chen, H., Wang, W., 2018. Netwalk: A flexible deep embedding approach for anomaly detection in dynamic networks, in: *SIGKDD*, pp. 2672–2681.
- Zhang, H., Wu, Q., Yan, J., Wipf, D., Yu, P.S., 2021. From canonical correlation analysis to self-supervised graph neural networks. *NeurIPS* 34.
- Zhang, Z., Wang, S., Ge, J., Xu, Y., Wu, Y., Wen, J., 2024. Graph anomaly detection via cross-layer integration, in: *2024 IEEE International Symposium on Parallel and Distributed Processing with Applications (ISPA)*, IEEE. pp. 710–717.
- Zhao, W., Guo, T., Yu, X., Han, C., 2023. A learnable sampling method for scalable graph neural networks. *Neural Networks* 162, 412–424.
- Zheng, Q., Xu, Y., Liu, H., Shi, B., Wang, J., Dong, B., 2023. A survey of tax risk detection using data mining techniques. *Engineering* .
- Zhou, T., Ye, H., Cao, F., 2024. Node-personalized multi-graph convolutional networks for recommendation. *Neural Networks* , 106169.
- Zhu, Y., Xu, Y., Yu, F., Liu, Q., Wu, S., Wang, L., 2020. Deep graph contrastive representation learning. *arXiv preprint arXiv:2006.04131* .
- Zhu, Y., Xu, Y., Yu, F., Liu, Q., Wu, S., Wang, L., 2021. Graph contrastive learning with adaptive augmentation, in: *WWW*, pp. 2069–2080.
- Zuo, Y., Liu, G., Lin, H., Guo, J., Hu, X., Wu, J., 2018. Embedding temporal network via neighborhood formation, in: *SIGKDD*, pp. 2857–2866.